Supporting information

Improved electrochemical performance of CoS_2/MWCNT nanocomposites for sodium ion batteries

Zulipiya Shadike[ab] ,Ming-Hui Cao[a], Fei Ding[b], Lin Sang[b], Zheng-Wen Fu[a*]

[a]*Shanghai Key Laboratory of Molecular Catalysts and Innovative Materials, Department of Chemistry & Laser Chemistry Institute, Fudan University, Shanghai 200433, P.R. China*

[b]*National Key Laboratory of Science and Technology on Power Sources,Tianjin Institute of Power Sources,Tianjin 300384, P. R. China*

EXPERIMENTAL SECTION

Preparation of CoS_2/MWCNT nanocomposites:CoS_2/MWCNT nanocomposites were synthesized by a simply hydrothermal method[1]. 2.5 mmol cobalt dichloride ($CoCl_2 \cdot 6H_2O$) and 2.5 mmol sodium thiosulfate ($Na_2S_2O_3 \cdot 5H_2O$) was dissolved in 30mL deionized water under the magnetic stirring at room temperature. Then 40 mg MWCNT was added into the solution. The overall volume of the mixture suspension was adjusted to 80mL by adding deionized water. After ultra-sonication and string for 3h, the mixture suspension was transferred into a 100ml Teflon-lined autoclave, sealed tightly, and heated at 180℃ for 12 h. After cooling naturally, the black precipitate was collected by centrifugation, washed with deionized water and ethanol several times, and dried at 80℃ in a vacuum oven overnight. For comparison, the CoS_2 samples were also prepared by above similar process without the presence of MWCNT in the solution.

Characterization: The crystal structure of as-synthesized CoS_2 and CoS_2/MWCNT samples were characterized by X-ray diffraction (XRD, BrukerD8 Advance, Germany) using Cu-Kα radiation (λ = 0.1540 nm) at 1.6Kw, Data were processed using the MDI-Jade version 7.0 software. Raman spectra were achieved on a LABRAM-1Bconfocal Raman spectrometer with 647.1nm radiation from an Ar–Kr laser. Thermo-gravimetric (TG) analysis was carried out on a (Pyris 1TGA) thermal analyzer with a heating rate of 10℃min^{-1}in flowing air atmosphere. Transmission electron microscope (TEM) and selected area electron diffraction (SAED) measurements were carried out by 200KV side energy JEOL 2010 TEM with energy dispersive X-ray (EDX) analyzers. For the *ex situ* measurements, to avoid the exposure to oxygen or water, care must be taken in the handling of samples at different states. The cell was disassembled in an Ar filled dry box and rinsed in anhydrous diglyme to eliminate residual salts then the active materials were rapidly transferred into the chambers.

For the electrochemical measurements, the working electrode consisted of active material (CoS_2 or CoS_2/MWCNT, 80 wt. %), electrical conductor (acetylene black, 10 wt. %), and binder (PVDF, 10 wt. %) on copper foil. The cells were assembled in an argon-filled glove box with the as-prepared materials as working electrode, and two sodium sheets as a counter and reference electrode, respectively. 1.0 M $NaClO_4$ (Aldrich) in a nonaqueous ethylene carbonate (EC)/propylene carbonate(PC) (1:1 in volume) and 1.0 M $NaCF_3SO_3$ (98%, Sigma-Aldrich) in diglyme ($(CH_3OCH_2CH_2)_2O$, anhydrous, 99.5%, Sigma-Aldrich) were selected as the electrolyte respectively. Galvanostatic charge-discharge cycles were carried out at room temperature with a Land CT 2001A battery test system. The cells were cycled between 1.0 and 2.9V vs. Na^+/Na. Cyclic voltammogram (CV) tests were performed on a CHI660A electrochemical working station (CHI instruments, TN).

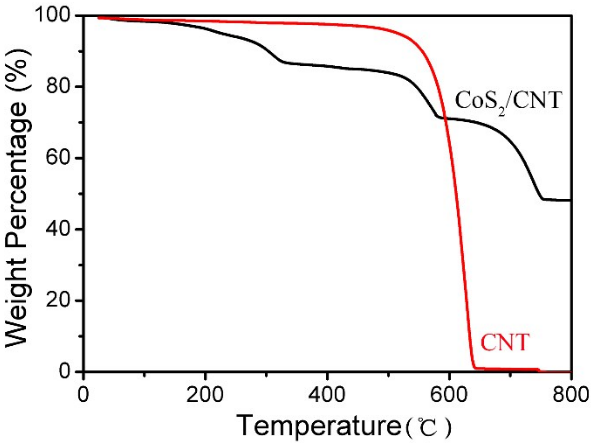

Figure S1 Thermogravimetric (TG) result of CoS_2/MWCNT and MWCNT in air with heating rate of 10℃min^{-1}.

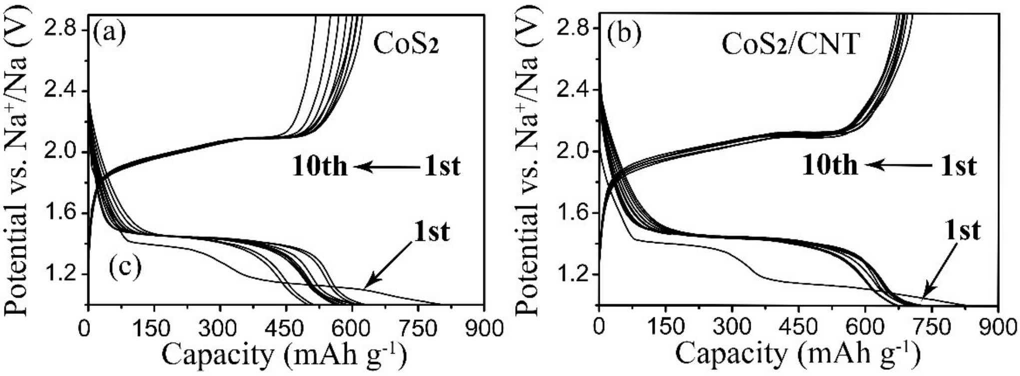

Figure S2 Discharge/charge curves of (a) CoS_2 and (b) CoS_2/MWCNT electrodes at a current density of 100 mA g^{-1}in 1 M $NaClO_4$-EC/PC.

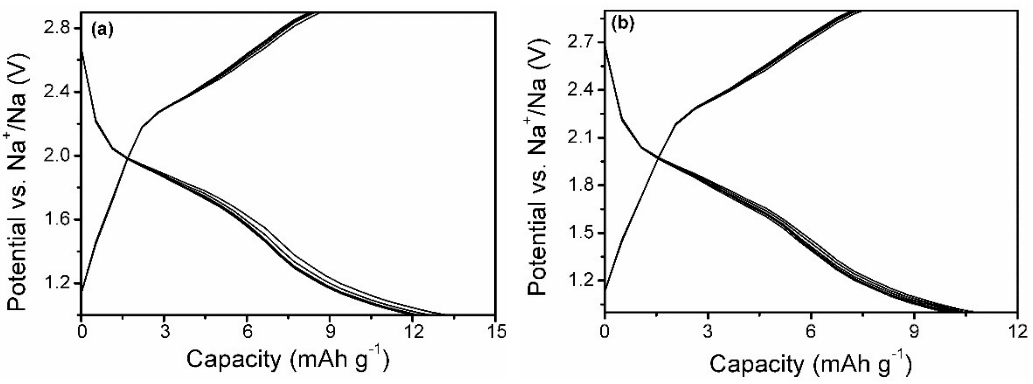

Figure S3 Discharge/charge curves of MWCNT electrodes at a current density of 100 mA g^{-1}in (a) 1.0 M $NaCF_3SO_3$-DGM and (b) 1.0 M $NaClO_4$-EC/PC.

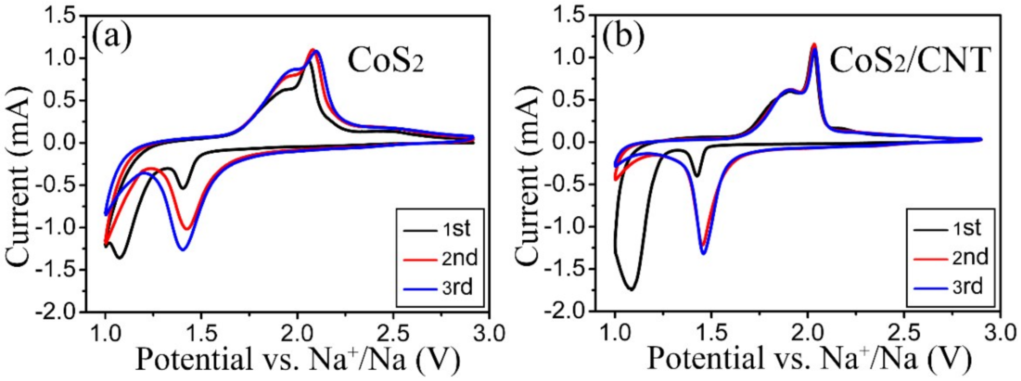

Figure S4 CV curves of (a) CoS_2 and (b) CoS_2/MWCNT electrodes between 1.0 and 2.9 V (vs. Na/Na^+) at the scan rate of 0.1 mV s^{-1}

Fig. S4 shows the cyclic voltammogram for CoS_2 and CoS_2/MWCNT electrodes at scan rate of 0.1 mV s^{-1} in the potential range of 1.0-2.9V. In the first cycle two reduction peaks at 1.1 and 1.4V and two oxidation peaks at 1.8 and 2.1 V are observed of both electrodes. The couple reduction/oxidation peaks may be related to multi-steps reaction mechanism. The reduction peak at 1.4V can be related to sodium insertion into CoS_2 forming Na_xCoS_2 and the peak at 1.1V can represents the conversion reaction forming Co and Na_2S.Whereas, in the subsequent cycles, these two couple of peaks for each cycle were almost overlapped, indicating that highly reversible reactions took place during the subsequent cycles.

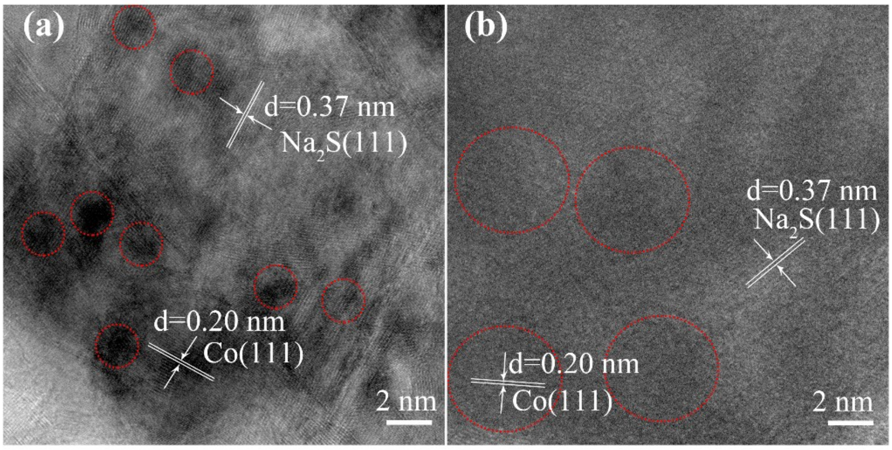

Figure S5 High-resolution TEM (HRTEM) images of sodiated electrodes (a) CoS$_2$/MWCNT and (b) CoS$_2$.

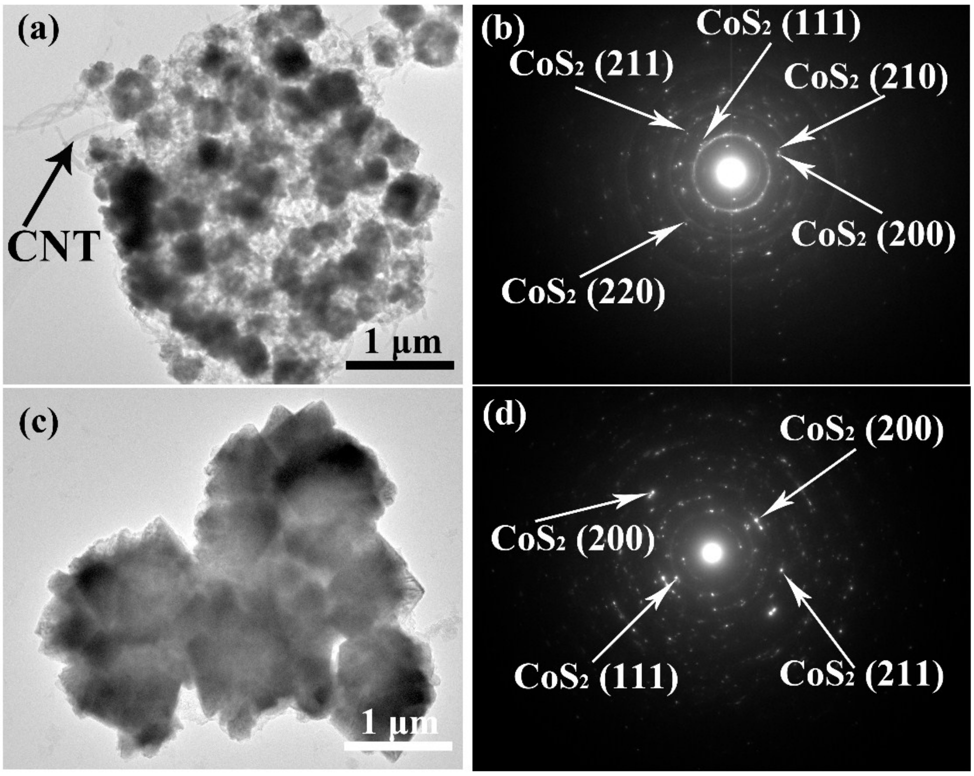

Figure S6 TEM images and SAED patterns of (a, b)CoS_2/MWCNT and (b)CoS_2 electrodes after charging to 2.9 V.

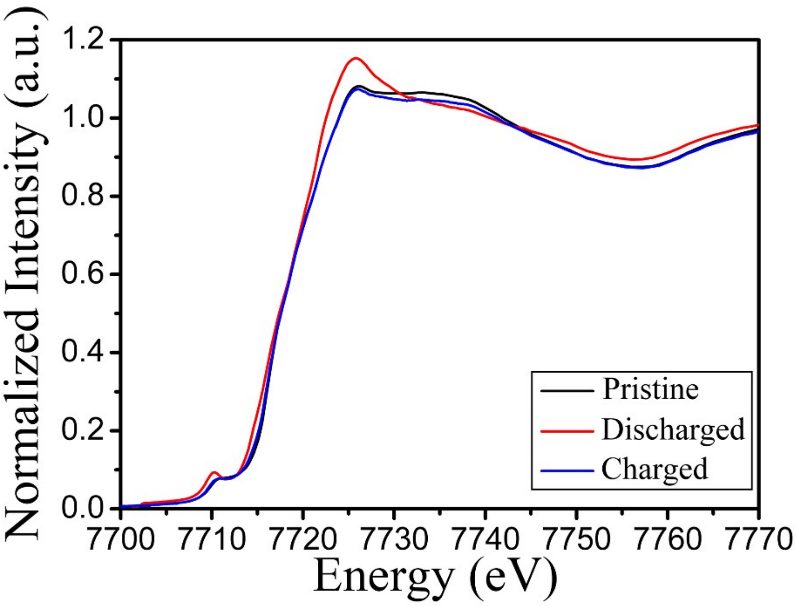

Figure S7 Co K-edge XANES spectra of pristine CoS_2 electrode (black line), after discharging to 1.0 V (red line) and charging to 2.9 V (blue line)

X-ray absorption spectroscopy was carried out to determine the variation in valence of Coin the sodiated and desodiated electrodes. Fig. S7 shows the Co K-edge XANES of the CoS_2 electrode after discharge to 1.0 V and recharge to 2.9 V, in comparing with the pristine sample. In the in initial state, the Fe K-edge absorption energy at 7714.7 eV could be assigned to Co^{2+} of CoS_2. After discharging to 1.0 V, the Co K-edge shifted to the lower energy, indicating the formation of Co after discharging process. After charging to 2.9 V, the corresponding Co K-edge shifted to higher energy and fully recovered to the original state as the pristine CoS_2.

Table S1 Sodium storage properties ofCoS_2 and other transition metal sulfides, oxides and selenides reported recently.

Materials	Curve shape	Discharge plateau voltage(V)	Second discharge capacity (mAh g^{-1})	Electrochemical Performance (mAh g^{-1})	Reaction mechanism	Reference
TiS_2	Platform	2.2	210	150(40th) at 0.04A g^{-1}	insertion	4
SnS	Platform	1.2	500	370(30th) at 0.125A g^{-1}	conversion	5
Cu_2S	Platform	1.0	260	261(20th) at 0.05A g^{-1}	insertion	6
Ni3S_2	Platform	0.9	370	250(40th) at 1C	conversion	7
MoS_2-C	Platform	1.0	500	390(100th) at 0.1A g^{-1}	conversion	8
WS_2	Slope	1.0	297	32 (500th) at 0.02A g^{-1}	conversion	9
WS_2/G	Slope	1.2	584	329(500th) at 0.02A g^{-1}	conversion	9
FeS_2	Slope	1.5-2.0	530	415(100th) at 0.06mAg^{-1}	conversion	11
FeS_2	Slope	1.5-2.0	250	170(2000th) at 1A g^{-1}	insertion	12
MoS_2/G	Slope	1.5	380	300(200th) at0.1A g^{-1}	conversion	S2
VS_2	Platform	1.8	70mAh	60mAh(22th)at0.5mAcm^{-2}	insertion	S3
$Nb_{1.1}S_2$	Platform	1.5	40mAh	26mAh(17th)at0.5mAcm^{-2}	insertion	S3
SeS_2	Slope	0.5-3.5	500	288(30th) at 0.1A g^{-1}	conversion	S4
CoS_2	Platform	1.4	724	194(100th) at 0.1A g^{-1}	conversion	T.W
CoS_2/CNT	platform	1.4	735	568(100th) at 0.1A g^{-1}	conversion	T.W
V_2O_5	Slope	2.5-3.5	180	170(20th) at 0.04A g^{-1}	insertion	S5
VO_2	Slope	2-3.7	200	150(50th) at 0.05A g^{-1}	insertion	S6
V_6O_{13}	Slope	2-3.0	170	120(30th) at 0.04A g^{-1}	insertion	S7
Fe_3O_4	Slope	1.8	140	90(35th) at 0.02A g^{-1}	insertion	S8
Alpha-MoO_3	Slope	1.4	210	116(500th) at 0.2C	conversion	S9
Fe_2O_3	Platform	1.0	580	385(200th) at 0.1A g^{-1}	conversion	S10
NiO	Platform	0.7	550	220(100th) at 0.1A g^{-1}	conversion	S10
Co_3O_4	Platform	0.75	450	180(100th) at 0.1A g^{-1}	conversion	S10
Mn_3O_4	Slope	1.3	157	120(100th) at 0.1A g^{-1}	conversion	S10
Sb_4O_2	Platform	0.9	900	724(20th) at 0.7C	conversion	S11
CuO bulk	Platform	0.75	280	53(50th) at 0.05A g^{-1}	conversion	S12
CuO nanowires	Platform	0.75	480	303(50th) at 0.05A g^{-1}	conversion	S12
TiO_2	Slope	2.0	90	150（15th） at 0.05A g^{-1}	insertion	S13
SnO_2/G	Slope	0.7-1.5	225	175(100th) at 0.02A g^{-1}	conversion	S14
SnO_2/NG	Slope	0.7-1.5	300	250(200th) at 0.08A g^{-1}	conversion	S14
Cu_2Se	Platform	1.9	200	114(100th) at 0.025 A g^{-1}	conversion	S15
VSe_2	Platform	1.6	48mAh	46mAh(24th)at1 μ Acm^{-2}	insertion	S16
$TiSe_2$	Slope	1.5	70mAh	65mAh(6th)at1 μ Acm^{-2}	insertion	S16
$MoSe_2$	Slope	0.7/2.1	108	65(8th) at0.25mAcm^{-2}	insertion	S17

*T.W=This Work; G:graphene; NG: nitrogen doped graphene ; CNT: carbon nanotube

Reference

[1] Z.D.Meng, L. Kefayat,U.Zhu, S.Ye, W.C.Oh,*Appl. Surf.Sci.*2013, *286*, 261–268.

[2] Y.X.Wang,S.L.Chou,W.David,H.K.Liu,S.X.Dou,*Chem. Eur. J.*2014, *20*, 9607 –9612.

[3] K.M.Abraham, L.Pitts, R.Schiff,*J. Electrochem. Soc*. 1980, 127 2545-2550.

[4] A.Ali, D.Damien, W. C.Karena,J. C.Peter,W.Weng,A.Khalil,*J. Am. Chem. Soc.*2012, *134*, 4505−4508.

[5] R.Vadivukarasi,R.Jordan,G.Cooper,W.Luo,X. F.Wang,F. S.William,D. S.Galen,X.L.Ji,*Nano Lett.*2014,

14, 4119−4124.

[6] W.Wang, B.Jiang, L.W.Hu,Z.H. Lin,J.G.Hou, S.Q.Jiao,*J. Power Sources*2014, *250*, 181-187

[7] H.L.Fei, Y. S.Lin, M.D.Wei, *J. Colloid Interf. Sci.*2014, *425*, 1–4.

[8] S.Komaba,T.Mikumo, A.Ogata,*Electrochem. Commun.*2008, *10,* 1276–1279.

[9] H.Srirama, S.Kuppan, B.Palani,*Electrochem. Commun.*2013, *31*, 5–9.

[10] Y. Z.Jiang,M.J.Hu,D.Zhang, T.Z.Yuan,W.P.Sun, B.Xu,M.Yan,*Nano Energy*2014, *5*, 60–66.

[11] Q.Sun,Q.Q.Ren,H.Li, Z.W.Fu,*Electrochem. Commun*. 2011, *13,* 1462–1464.

[12] L.J.Wang,K.Zhang,Z.Hu,W.C.Duan,F.Y.Cheng, J.Chen,Nano *Res.*2014, 7, 199-209.

[13] H.Xiong, D.Michael,M. B.Slater,S. J.Christopher, R.Tijana,*J. Phys. Chem. Lett.*2011, 2, 2560–2565.

[14] X.Q.Xie,D.W.Su,J.Q.Zhang,S.Q.Chen,K. Manjon, G.X.Wang,*Nanoscale*2015, *7*, 3164–3172.

[15] J.L.Yue,Q.Sun,Z.W.Fu, Chem. *Commun.*2013, *49*, 5868—5870

[16] K. Abraham, L.Pitts,*J. Electroche. Soc.*1981, *128*, 1060-1062.

[17] J.Morales, J.Santos,J.L.Tirado,*Solid State Ionics*, 1996, *83*, 57-64.